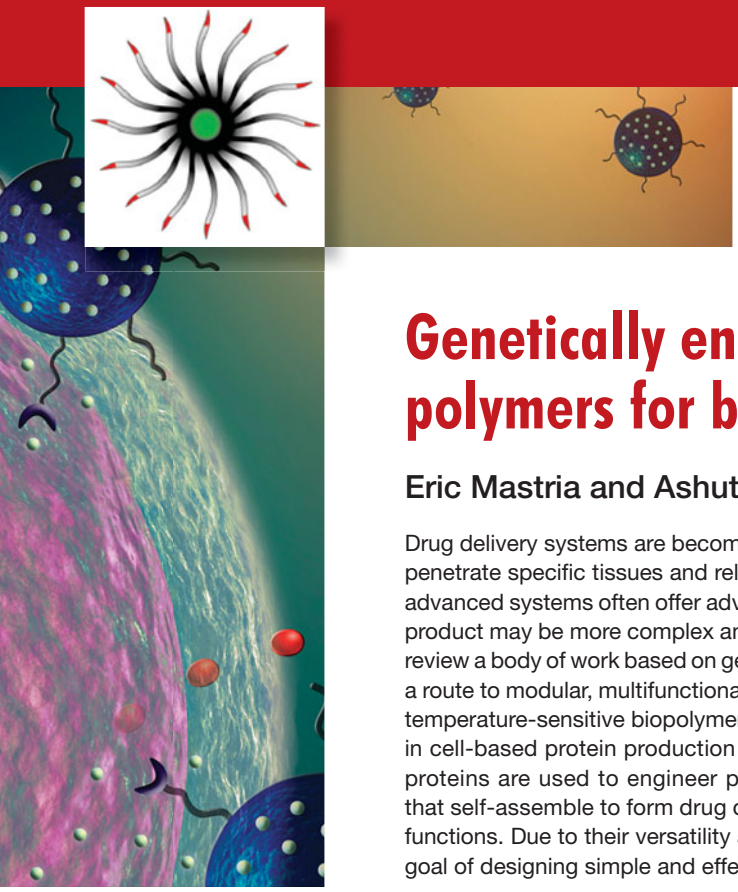


Genetically encoded "smart" peptide polymers for biomedicine

Eric Mastria and Ashutosh Chilkoti

Drug delivery systems are becoming increasingly sophisticated, with the ability to target and penetrate specific tissues and release drugs based upon the local environment. While these advanced systems often offer advantages over their less sophisticated counterparts, the final product may be more complex and require additional manufacturing steps. In this article, we review a body of work based on genetically encoded elastin-like polypeptides (ELPs) that offer a route to modular, multifunctional delivery systems that are simple to manufacture. ELPs are temperature-sensitive biopolymers that can be designed on the genetic level and expressed in cell-based protein production systems. The tools of molecular biology and versatility of proteins are used to engineer polymers with precise composition and molecular weight that self-assemble to form drug delivery systems with an impressive variety of features and functions. Due to their versatility and ease of production, ELPs are likely to contribute to the goal of designing simple and effective "smart" delivery systems.

Design of drug delivery systems

Many drugs fail to meet their therapeutic potential because they do not attain a sufficient concentration in the tissue of interest without causing off target effects.[1,2] For this reason, there has been great interest in enhancing the delivery of drugs to the site of interest while reducing their concentration at off target sites.[3–5] Early approaches to do so included altering a drug's solubility, plasma half-life (the time required for a drug's concentration in the plasma to decrease by a factor of two), and biodistribution with liposomal nanoparticle drug formulations (amphiphilic lipids that can entrap drugs).[6–8] To gain further control over the behavior of drug delivery systems, researchers have incorporated ligands to target specific cells or materials that could sense changes in environment (pH, temperature, etc.) and unload their cargo at the site of interest.[9–13] While these approaches often lead to improved *in vivo* performance, these systems have multiple components that must be separately synthesized and then combined into a delivery system, increasing the eventual cost and complexity of the resulting product.

An emerging alternative is to use genetically encoded polypeptides.[14–16] With this approach, most if not all of the desired functionality can be designed at the DNA level and then expressed as a fusion polypeptide that contains different structural and functional domains of interest, such as drug conjugation, cell targeting, environmental sensitivity, cell uptake, and intracellular trafficking.[16–19] In this review, we describe how drug delivery systems with these features can be produced using elastin-like polypeptides (ELPs).

Development of genetically encoded drug delivery systems

ELPs are a versatile platform technology for genetically encoded drug delivery systems.[20] Derived from the peptide sequence found in the hydrophobic domain of human tropoelastin (the precursor to the protein elastin found in connective tissue), they consist of repeats of the pentapeptide motif VPGXG, where X is any amino acid other than proline, V is valine, P is proline, and G is glycine.[20] ELPs exhibit lower critical solution temperature (LCST) phase behavior in aqueous solvents. For a given molecular weight (MW), composition (identity of X), concentration, and cosolutes, each ELP has a distinct cloud point temperature (T_t), below which the ELP is soluble, and above which it reversibly aggregates into a polymer rich coacervate phase.[20,21] The phase transition can also be triggered isothermally by increasing the concentration of salts;[20] the propensity of salts to trigger the phase transition follows the Hofmeister series, which is an ordering of ions according to their ability to precipitate proteins.[22] This environmental sensitivity is critical to the utility of ELPs: their reversible responses ease protein purification and confers

Eric Mastria, Duke University, Durham, NC; eric.mastria@duke.edu
Ashutosh Chilkoti, Department of Biomedical Engineering, Duke University, Durham, NC; chilkoti@duke.edu
DOI: 10.1557/mrs.2013.313

© 2014 Materials Research Society

https://doi.org/10.1557/mrs.2013.313 Published online by Cambridge University Press

environmental sensitivity to ELP-based drug delivery systems. Because their physical properties—MW and composition—can be precisely controlled at the genetic level, ELPs can be tuned to have a specific T_t. Increasing the MW and the hydrophobicity of the X residue decreases T_t.[23] At the same time, manipulating the MW and composition also affects the *in vivo* behavior of an ELP. For example, the MW can be manipulated to achieve the desired *in vivo* half-life.[24]

ELPs can also be expressed as block copolymers to drive their self-assembly into nanoparticles and can be fused with peptides that confer site-specific reactivity that enables drugs or imaging agents to be attached at specified sites along the polypeptide chain or that confer biological activity to the ELP, such as receptor targeting or cell uptake.[25–27] Their T_t can be tuned to be responsive in the temperature range of 39–42°C, triggering their transition into microscopic aggregates or nanoscopic micelles within the vasculature of tumors. This temperature range is critical because it has been applied to human patients in clinical hyperthermia treatments.[19,28]

By using the tools of molecular biology, it is relatively simple to design and express an ELP fusion to meet many of the design criteria for nanocarriers, namely they (1) are easily produced in a scalable manner, (2) are composed of nontoxic materials, (3) self-assemble—when designed to do so—into a monodisperse population of nanoparticles, (4) target the desired anatomical site and unload drugs with the appropriate kinetics at that site, and (5) are flexible enough to deliver a wide array of drugs. Because of these attributes, ELPs provide a platform that, we believe, will promote the facile development of the next generation of genetically engineered drug delivery systems.[29,30]

Expression and purification of ELPs from *E. coli*

ELPs are typically synthesized in *E. coli*—though other organisms can, and have, been used to produce ELPs.[31] To do this, the DNA encoding of an ELP is cloned into an expression plasmid that contains genetic regions conferring antibiotic resistance and promoting transcription. *E. coli* are induced to take up the DNA in a process called transformation, and colonies containing the foreign DNA are picked on the basis of antibiotic resistance. For reasons that are not totally clear, *E. coli* produces most ELPs with high yield, even in low-density shaker flask fermentation (~50–500 mg/L of culture, depending on the construct). This high level of expression is important because some recombinant polypeptides are plagued by poor expression, which makes purification of the molecule difficult and increases the cost of the final product. Their thermal responsiveness is the second useful attribute that greatly facilitates their purification. Their aggregation upon heating above T_t is completely reversible such that ELPs dissolve when the solution temperature is decreased below their T_t. Importantly, this process occurs even in complex mixtures such as *E. coli* lysate, which are cells that have been lysed open by sonication or other means. Thus, by triggering the phase transition repeatedly with heat and/or salt, ELPs (along with the protein they are genetically fused to) can be purified from cell lysate without chromatography, a process named inverse transition cycling (ITC). As shown in the SDS-PAGE (sodium dodecyl sulfate polyacrylamide gel electrophoresis) gel in **Figure 1**a, just two rounds of ITC yield a highly pure product.[32] Lane 1 shows the soluble proteins found in the *E. coli* lysate, including the desired ELP product in the dark band at a MW of ~55 kilodaltons (kDa) indicated by an arrow. The soluble lysate is heated, and salt is added in order to trigger the ELP phase transition. The dense ELP aggregate is then separated from soluble contaminating proteins by centrifugation. Lane 2 shows the supernatant, containing contaminating proteins and only a trace of ELP product, while Lane 3 is the pellet resolubilized in cool, low salt buffer, containing ELP product and no obvious contaminating

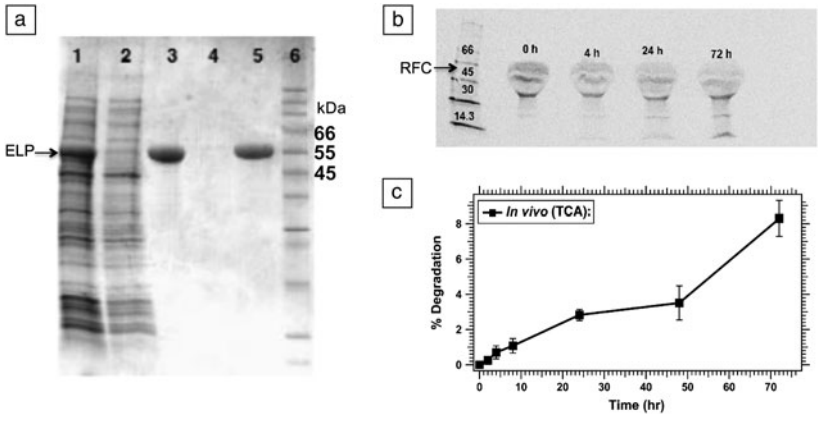


Figure 1. Purification and biodegradability of elastin-like polypeptides (ELPs). (a) Purification of an ELP-thioredoxin fusion protein by inverse transition cycling. The purification is followed by running samples from each step on a SDS-PAGE (sodium dodecyl sulfate polyacrylamide gel electrophoresis) gel. Lane 1: Soluble *E. coli* lysate. The ELP-fusion protein is visible at approximately 55 kilodaltons (kDa), marked by an arrow. Lane 2: Supernatant from first hot spin, demonstrating that most non-ELP proteins remained soluble. Lane 3: Resolubilized hot spin 1 pellet, where the ELP-thioredoxin fusion is the band near 55 kDa. Lane 4: Hot spin 2 supernatant, which is largely free of contaminating protein. Lane 5: Hot spin 2 with highly pure ELP-thioredoxin protein, with no detectable bands from contaminating proteins. This is the final product of the purification process. Lane 6: Molecular weight (MW) ladder, with bands labeled in kDa. (b) *In vitro* biodegradability of ELP. Breakdown of ^{14}C-labeled ELP after incubation in fresh mouse serum at 37°C. The MW is indicated by the MW marker in the left lane shown in kDa. An arrow demarcating the approximate renal filtration cutoff (RFC) is included for reference. The incubation time is indicated above each sample. The distended appearance of the ELP band (top band) is due to the presence of serum albumin in plasma at a similar MW (~67 kDa). (c) After tail vein injection of mice bearing FaDu tumors (a cell line derived from human squamous cell carcinoma of the pharynx), percent degradation was calculated as measured by TCA (trichloroacetic acid) precipitation. Reproduced with permission from Reference 24, © 2006 Elsevier and Reference 32, © 1999 Nature Publishing Group.

https://doi.org/10.1557/mrs.2013.313 Published online by Cambridge University Press

protein bands. The process is repeated, where Lane 4 is the supernatant, and Lane 5 is the ELP pellet. Lane 6 contains MW standards, labeled in kilodaltons (kDa). This example is typical of ELP purification, where 2–3 rounds of ITC remove all detectable contaminating proteins according to SDS-PAGE.

Biodegradability of ELPs

Many drug delivery systems are composed of synthetic molecules that are often not biodegradable.[30,33] To avoid material accumulation, especially upon repeated administration, their molecular weight must be restricted to below the renal filtration cutoff (~60 kDa or ~5–6 nm) such that they can be excreted through the kidneys.[30,34–36] While this size limit avoids toxicity because of unwanted accumulation in healthy organs, especially the kidney, liver, and spleen, which are the major organs involved in clearing materials out of the body, it also sets a limit to their performance as a drug delivery system. The main reason that macromolecular carriers outperform free drugs in the treatment of cancer is that they are designed to have a size above the renal filtration cutoff but well below the pore size (400–600 nm) in the leaky tumor vasculature in order to be passively taken up by a tumor.[37] An advantage of genetically engineered polymers such as ELPs is that they are biodegradable. As shown in Figure 1b, an ELP incubated in plasma broke down, leading to smaller MW bands that are below the renal filtration cutoff (RFC) appearing over time. In Figure 1c, ELP injected intravenously broke down *in vivo* at a rate of ~2.5% per day. Because of this biodegradability, ELPs can be administered at a molecular weight above the renal filtration cutoff, circulate for an extended period of time, and are eventually broken down into smaller fragments that are cleared through the kidneys.[24]

Finely tuned and reliably predicted ELP transition temperatures

A useful attribute of genetically encoded polymers such as ELPs is that their composition and MW can be precisely controlled at the gene level, leading to precise tuning of the T_t of an ELP.[23] However, the number of possible ELPs that *exhibit* a given T_t is enormous because of the large number of options in the choice of the X residue. To constrain the design space, McDaniel and Chilkoti systematically explored ELPs that were composed only of the amino acids alanine and valine at the guest residue (Xaa, 4th position) of the pentapeptide sequence.[23] An analytical equation (Equation 1) that predicts T_t as a function of the fractional alanine content, the chain length of the ELP (*length*) and the ELP concentration (*conc*), was developed as follows:[23]

$$T_t = A\,e^{B f_{alanine}} + \frac{C\,e^{D f_{alanine}}}{length}\left[\ln(E) + F f_{alanine} - \ln(conc)\right], \quad (1)$$

where A–F are non-zero constants, and $f_{alanine}$ represents the ratio of alanines to the total number of guest residue positions. This analytical equation is useful because it enables *de novo* prediction of the amino acid sequence and chain length of ELPs that will display a desired T_t in a physiological buffer within a specified concentration regime, thereby greatly facilitating the design of new ELPs. This family of ELPs covers a large range of transition temperatures (~20–140°C) and MWs (~10–65 kDa). **Figure 2**b shows that this model is highly robust, as it predicts the T_t of other ELPs, which were not included in the model. While this is a simplified model, in that it only allows valine and alanine as the guest residues, this model can be extended to other families of ELPs with different residues at the guest position in the VPGXG repeat and clearly demonstrates how precise control of composition and MW can be used to design an ELP with the desired T_t.

ELPs conjugate to hydrophobic molecules to form nanoscale micelles

ELPs can be expressed with cysteine (Cys) residues at desired locations in the protein in order to allow the attachment of small molecules by reaction with thiol-reactive moieties; other reactive residues such as lysine, tyrosine, serine, threonine, aspartic, or glutamic acid can be similarly used. Mackay and co-workers designed a polymer that they termed a chimeric polypeptide (CP) that consists of two domains: a water soluble ELP with a T_t >> 37°C that is hence highly soluble at body temperature and does not contain any Cys residues, and a short "attachment segment" that consists of

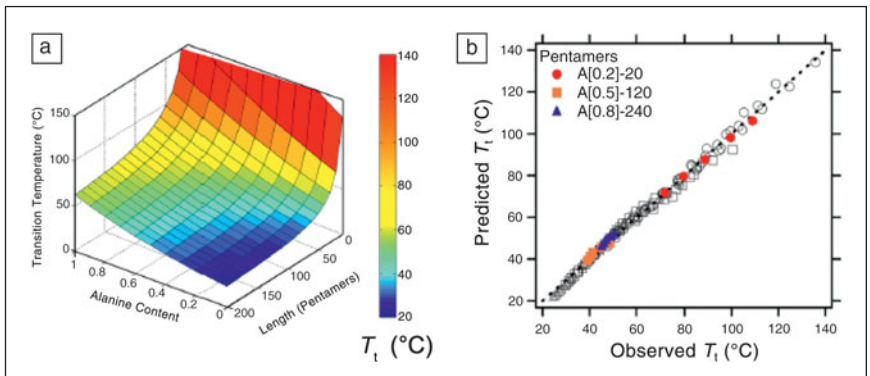


Figure 2. Elastin-like polypeptide (ELP) transition temperatures can be predicted by an analytical model. (a) Three-dimensional surface plot of T_t (cloud point temperature) versus $f_{alanine}$ (fraction of alanines in guest residue positions) versus pentamer repeats at 25 μm in phosphate buffered saline. The cloud point temperature tends to increase with an increase in $f_{alanine}$ and a decrease in the number of pentamer repeats. (b) Demonstration of model fit (dotted line) by plotting observed versus predicted T_t. Unfilled data points were used in developing the model and led to a coefficient of determination (R^2) value of 0.993. Colored points are ELPs made subsequent to the development of the model and fall very close to the model's prediction (R^2 = 0.999, slope = 0.95). The red circles (A[0.2]-20) contain 20% alanine in the guest residue position, with 20 pentamer repeats. The orange squares (A[0.5]-120) contain 50% alanine in the guest residue position with 120 pentamer repeats. The blue triangles (A[0.8]-240) contain 80% alanine in the residue position, with 240 pentamer repeats. Adapted with permission from Reference 23.

https://doi.org/10.1557/mrs.2013.313 Published online by Cambridge University Press

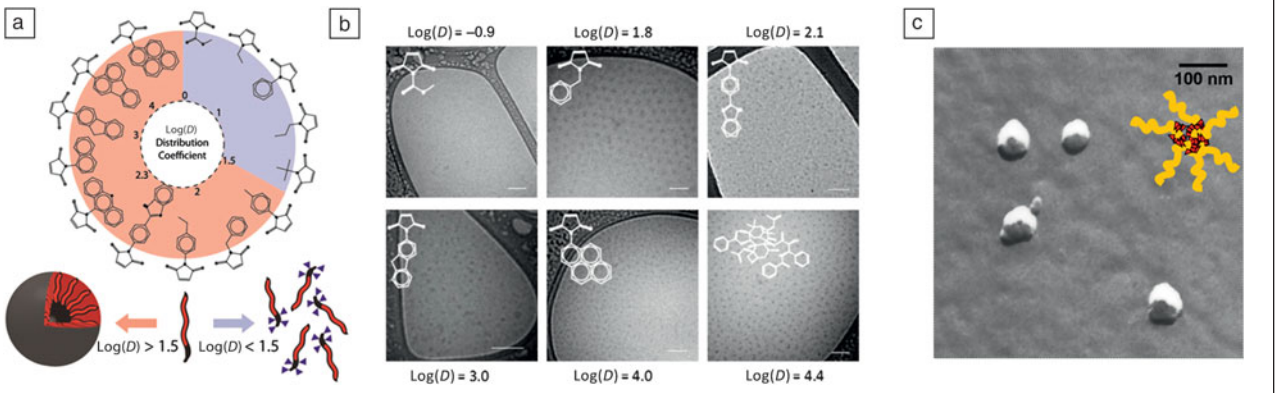


Figure 3. Elastin-like polypeptides (ELPs) self-assemble into micelles upon conjugation of hydrophobic molecules. (a) Schematic showing range of molecules tested and the cutoff for micelle formation. The compounds all share a functional group for conjugation to cysteine as a maleimide bond, shown outside the circle. The compounds begin at the top of the circle with relatively hydrophilic molecules that steadily increase in hydrophobicity as measured by the Log of the octanol-water distribution coefficient (Log(*D*)). The attachment of compounds with Log(*D*) < 1.5 (shown in blue) did not trigger self-assembly of the chimeric polypeptide (CP), whereas compounds with Log(*D*) > 1.5 (shown in pink) triggered self-assembly of the CP into nanoparticles. (b) Cryo-TEM (cryogenic transmission electron microscopy) images of CP conjugates, confirming cutoff of 1.5 for Log(*D*). Scale bars: 100 nm. (c) Freeze-fracture TEM of chimeric polypeptide-doxorubicin (CP-Dox) micelles, showing nanoparticles with a size of ~50 nm. Inset at top right of panel shows a schematic of star-like micelle, with hydrophobic doxorubicin (red) in the core and hydrophilic ELP (yellow) in the corona. Adapted from with permission from References 17 and 38.

a Cys[Glycine-Glycine-Cys]$_7$ segment at the carboxy terminus of the ELP.[38] McDaniel et al. attached a set of maleimide derivatives with a wide range of hydrophobicity to the CP and found that when the attached molecule is sufficiently hydrophobic, the CP self-assembles into spherical micelles with a diameter of 40–60 nm. McDaniel et al. showed that the cutoff for micelle formation lies at 1.5 for the Log of the octanol-water distribution coefficient (Log(*D*)).[38] As shown in **Figure 3**a, molecules with a Log(*D*) greater than 1.5 form micelles as visualized by cryogenic transmission electron microscopy (cryo-TEM) (Figure 3b).[38]

The conjugation-triggered self-assembly of CPs was exploited to develop a nanoscale delivery vehicle for the cancer chemotherapeutic doxorubicin (Dox).[17] To ensure intracellular release of the drug, doxorubicin was modified by reaction with *N*-beta-Maleimidopropionic acid hydrazide (BMPH) that contains an internal acid-labile hydrazone bond. The terminal maleimide moiety on the modified drug was attached to the cysteine residues in the CP.[17] As shown in the freeze fracture TEM image in Figure 3c, the ELP-drug conjugate self-assembles into near-monodisperse micelles approximately 50 nm in diameter. The use of the genetically engineered ELP has several advantages for this application. First, the attachment sites can be precisely clustered on one end of the polymer, driving micelle formation.

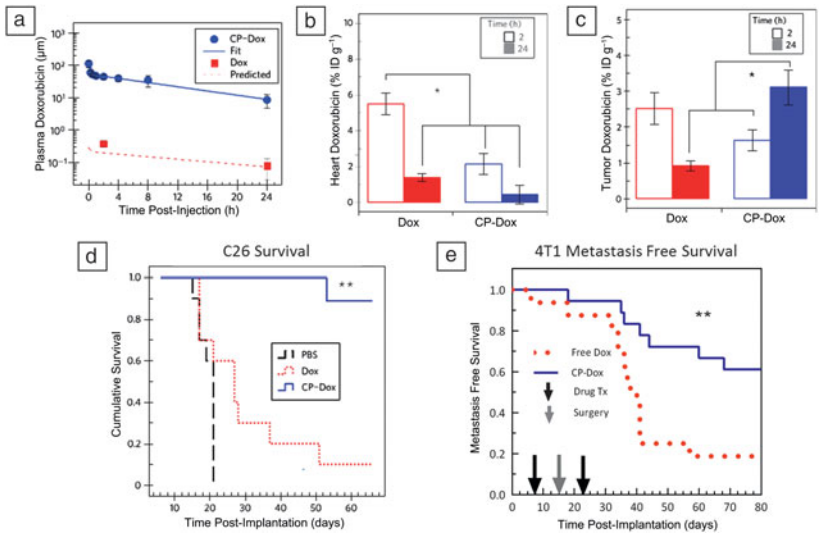


Figure 4. Conjugation of doxorubicin to elastin-like polypeptide (ELP) improves its efficacy in comparison to free doxorubicin. (a) Pharmacokinetics of chimeric polypeptide-doxorubicin (CP-Dox) and free doxorubicin demonstrating higher plasma levels and longer half-life of CP-Dox than free drug. The data closely follow the two-compartment model fit applied to the CP-Dox data (Fit), and to the predicted pharmacokinetic model of free Dox in mice (Predicted). (b) Significantly lower accumulation of doxorubicin in the heart for CP-Dox treated mice. (c) Significantly higher accumulation of doxorubicin in a subcutaneous C26 tumor for CP-Dox mice (for b and c, * indicates $p < 0.0005$, where p is the result from any statistical test, which represents the probability that the results observed were due to random chance) (analysis of variance, Tukey's Post-hoc test). (d) Significantly improved survival of CP-Dox treated mice for subcutaneous C26 tumor bearing mice (** indicates $p = 0.0001$, 0.00004 for CP-Dox versus Dox and phosphate buffered saline (PBS, vehicle control), respectively (Kaplan–Meier)). (e) Mice were inoculated orthotopically with 4T1 murine mammary tumor on Day 0. Mice treated with neoadjuvant and adjuvant CP-Dox treatment (Drug Tx-drug treatment, black arrows) along with surgery (gray arrow) had significantly prolonged metastasis-free survival compared to free Dox mice (** indicates $p < 0.01$, Log-Rank test). Adapted from Reference 17.

https://doi.org/10.1557/mrs.2013.313 Published online by Cambridge University Press

Second, the number of attachment sites can be precisely controlled, enabling control of drug loading. This is advantageous in comparison to synthetic polymers, which may have only one reactive group at the end of the polymer. Third, this approach decouples the loading and unloading process of the drug, so that drug release can be triggered by changes in its local *in vivo* environment. The particles taken up by endocytosis enter endosomes, which then fuse lysosomes, where the pH is acidified to ~5, and this environment hydrolyzes the hydrazine bond, releasing the drug.

Enhanced efficacy of ELP-drug conjugates compared to free drug

The chimeric polypeptide-doxorubicin conjugate, termed CP-Dox, demonstrates greatly improved performance in syngeneic murine tumor models, which are tumors that can be transplanted and grown in inbred strains of mice with normal immune systems.[17] Compared to the free drug (Free Dox), CP-Dox micelles have a higher maximum tolerated dose (20 mg/kg versus 5 mg/kg), a longer plasma half-life, increased accumulation in the tumor, and decreased accumulation in the heart (the organ that experiences dose-limiting toxicity in doxorubicin treatment) (**Figure 4**a–c).[17] These improved performance metrics translate into a significant improvement in survival in the C26 cell line, a syngeneic murine colon carcinoma model for the Balb/C strain of mice (Figure 4d). A single dose of CP-Dox leads to complete tumor regression and cures in ~90% of mice.[17]

Treatment with CP-Dox was also tested in mice bearing the 4T1 cell line, a syngeneic murine mammary (breast) carcinoma model for the Balb/C strain of mice that is known to be refractory to doxorubicin treatment.[39] When given as a neoadjuvant treatment one week before surgical removal of the primary tumor and again as an adjuvant treatment a week after surgery, CP-Dox significantly improved metastasis free survival over free doxorubicin ($p < 0.01$, Log-Rank test, where p is the result from the statistical test and represents the probability that the results observed were due to random chance, Figure 4e).

Design of CP-Dox nanoparticles that aggregate upon the application of mild hyperthermia

Mild hyperthermia in solid tumors, where the mean temperature is maintained at ~42°C, has been shown to be synergistic with external beam irradiation.[40] Because ELPs are thermally responsive, endowing CP-drug nanoparticles with thermal responsiveness in the proper temperature range—such that they aggregate in tumors that are heated to 42°C—potentially offers a means to thermally target them to tumors. However, the CP-Dox nanoparticles described previously are not thermally responsive in the relevant temperature range of 38–42°C. To develop the next generation of thermally targeted CP-Dox nanoparticles, MacDaniel et al. re-engineered the composition and chain length of the ELP segment of the CP such that the CP-Dox nanoparticles aggregate in response to mild hyperthermia.[41] This next-generation thermally responsive CP-Dox conjugate forms ~40 nm diameter nanoparticles that are stable at body temperature and display a nanoparticle-to-aggregate phase transition between 39–42°C in media, a temperature range suitable for mild hyperthermia of solid tumors (**Figure 5**a). The phase transition is tracked by an increase in optical density, because the insoluble ELP scatters light. The CP-Dox nanoparticle is stable upon dilution to low micromolar concentrations and is cytotoxic at both 37°C and 42°C (Figure 5b–c).

An additional finding, which is crucial for the application of this system *in vivo*, is that the T_t of CP-Dox micelles is far less dependent on concentration than that of ELP unimers (ELP molecules in solution that are not assembled into any nanostructure) (Figure 5d). This means that over a large concentration range (and therefore over a long period of time post-IV [intraveneous] injection), the T_t of the micelles remains within the narrow 37–42°C range,

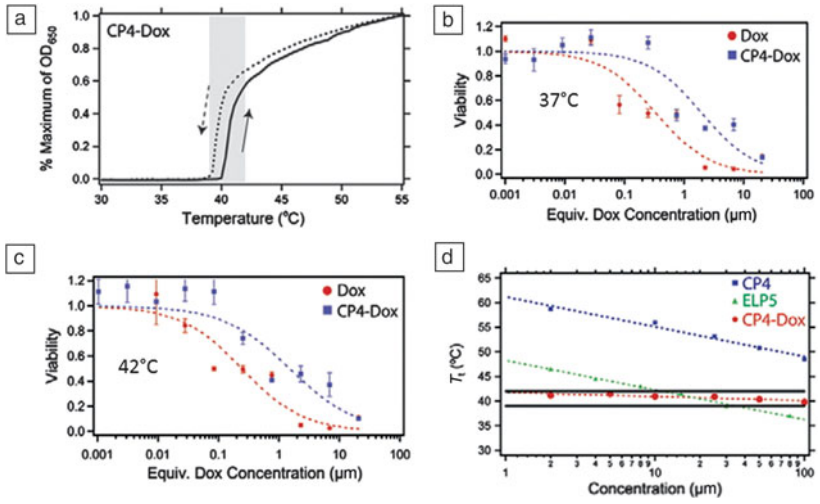


Figure 5. Doxorubicin nanoparticles that transition upon application of mild hyperthermia. (a) Chimeric polypeptide-doxorubicin (CP-Dox) nanoparticle is designed to transition sharply between 39°C and 42°C (the range relevant for clinical hyperthermia, shaded in gray), leading to an increase in the optical density (OD) as the temperature of the solution increases. Cytotoxicity of the drug conjugate is consistent whether cells were kept at (b) 37°C or (c) 42°C, as measured by viability (fraction viable compared to untreated control). (d) The formation of micelles keeps the local concentration of elastin-like polypeptide (ELP) relatively constant even for bulk changes in concentration, leading to near-independence of the T_t on bulk concentration. As shown by the horizontal lines on the graph, the transition temperature of the CP-Dox nanoparticle (red) remains in the relevant temperature range of 37–42°C over a concentration range spanning three orders of magnitude. In contrast, the same ELP without doxorubicin attached (CP4, blue) and another ELP (ELP5, green) in unimer form, show strong dependence of T_t (cloud point temperature) on concentration. Adapted from Reference 41.

https://doi.org/10.1557/mrs.2013.313 Published online by Cambridge University Press

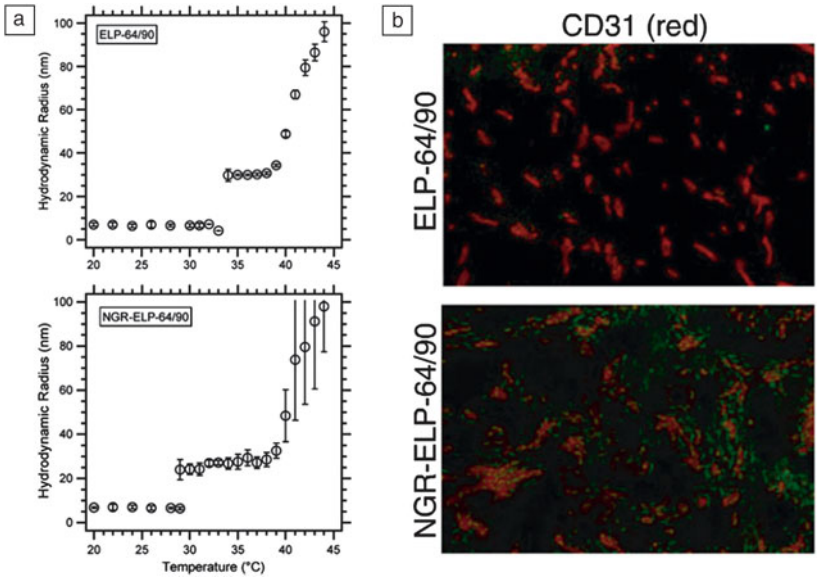


Figure 6. Targeting tumor endothelial cells with NGR (Asparagine-Glycine-Arginine) presenting elastin-like polypeptide (ELP) micelles. (a) ELP block copolymers assemble to form ~50–60 nm diameter spherical micelles at body temperature without NGR peptide (top) and with NGR peptide (bottom), as measured by dynamic light scattering. (b) Confocal microscopy of tumor tissue after tail vein injection of fluorophore-labeled micelle-forming ELP diblock copolymers. The NGR presenting micelles (NGR-ELP-64/90, bottom) are seen at a much higher density compared to the ELP control without ligand (top). The ELP (green) co-localizes with the CD31 antibody, which stains endothelial cells (red). Adapted from Reference 42.

such that the micelles remain thermally responsive upon dilution.[41]

Micelle formation by self-assembly of ELP block copolymers

The unique properties of ELPs allow the genetically encoded synthesis of temperature-responsive micelles, even without the conjugation of a hydrophobic small molecule. This can be done by designing a diblock with a hydrophobic and hydrophilic ELP segment.[26] Unlike most synthetic polymer amphiphiles that consist of two segments with different monomers, both segments of diblock ELPs are composed of VPGXG repeats, with the only difference being the choice of the guest residue (X) in the two blocks. By selecting guest residues (X) with significantly different hydrophobicities, a diblock ELP can be designed that is highly water soluble below a critical temperature but undergoes selective desolvation of the more hydrophobic block with an increase in temperature. Above this critical temperature—defined as the critical micellization temperature (CMT)—the ELP gains enough amphiphilicity to spontaneously self-assemble into spherical micelles as measured by dynamic light scattering[26] (**Figure 6**a). With a further increase in temperature, the more hydrophobic block also desolvates, and at a critical temperature, the micelles transition to an insoluble aggregate.[26]

This architecture has many strengths but also some limitations. First, it allows one to design temperature responsive polymer amphiphiles with a CMT that can be varied across a range of temperatures. Unfortunately, although the T_t of each ELP segment in a diblock copolymer can be precisely predicted individually, the CMT for the fusion is much more difficult to predict. Despite this limitation, through trial-and-error, we have succeeded in designing diblock ELPs that display thermal responsiveness in different temperature regimes of interest, as described later.

Ligand targeting with ELP micelles

Diblock ELPs can be expressed as fusions with peptide ligands. By appending the ligand on the terminus of the hydrophilic block (e.g., ligand-hydrophilic-hydrophobic segment), the ligand is presented on the corona of the micelle. In a study by Simnick et al., an ELP diblock copolymer was fused with the NGR amino acid sequence (N-Asparagine, G-Glycine, R-Arginine), a ligand for CD13.[42] CD13 is upregulated on the membranes of endothelial cells (the cells that line the lumen of blood vessels) that are angiogenic (producing new blood vessels). Fast-growing tumors continually grow new blood vessels to provide nutrients, and therefore CD31 is overexpressed on the endothelial cells of many tumors.[43,44] As shown in Figure 6a, the incorporation of the NGR peptide at the N-terminus of the ELP block copolymer does not disrupt their self-assembly, as both the NGR containing and ligand-free ELP block copolymer exist as 50–60 nm diameter micelles at body temperature. When injected in mice bearing FaDu tumors (a cell line established from a human squamous cell carcinoma of the pharynx), the NGR functionalized block copolymer (green, Figure 6b) shows greater accumulation within the tumor than the control ELP that does not present the peptide. The NGR functionalized micelles co-localize with the endothelial cell marker CD31 (red).

Temperature triggered micelle formation to improve cell uptake

The CMT of ELP block copolymers can also be tuned to occur at temperatures relevant to applied hyperthermia (37°C < CMT < 42°C). If the transition takes place in this range, then the ELPs can be triggered to form micelles in any tissue that is externally heated to ~42°C. This approach opens up the possibility of new sets of ligands that do not bind tightly when presented in single form but are "activated" by being presented at high density.[45,46]

Proof-of-principle of this approach was demonstrated by Simnick et al. in a study in which the arginine-glycine-aspartate (RGD) peptide was displayed on the N-terminus of an ELP block copolymer that was designed to exhibit a CMT between 37°C and 42°C (**Figure 7**a). The RGD peptide binds

https://doi.org/10.1557/mrs.2013.313 Published online by Cambridge University Press

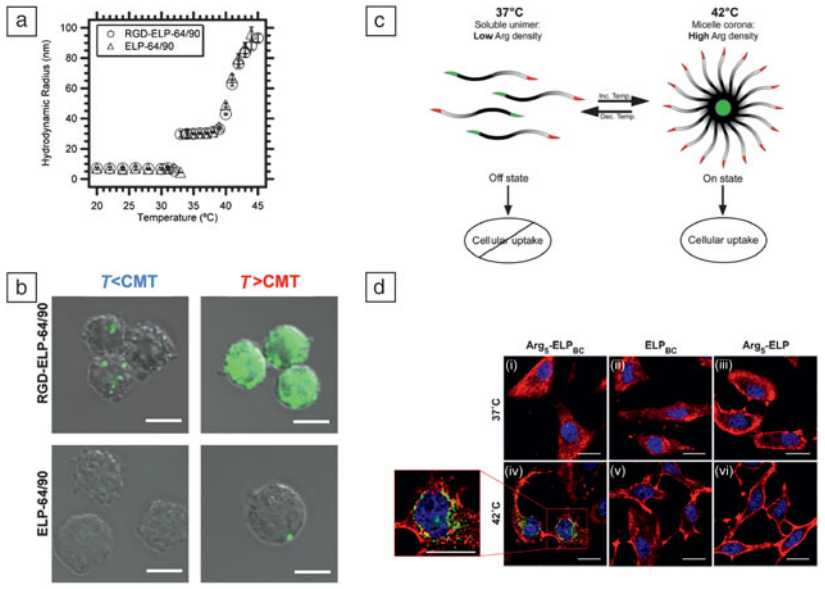


Figure 7. Intracellular targeting with temperature triggered elastin-like polypeptide (ELP) micelles. (a) Dynamic light scattering data showing a sharp transition from unimer to micelle (critical micellization temperature [CMT] between 33°C and 34°C) for ELPs with and without the RGD (Arg-Gly-Asp) ligand. (b) Cell uptake, indicated by increased intracellular green signal, is triggered by incubation above the CMT with micelles that are decorated with RGD ligand (top right). Uptake is poor for temperatures below the CMT (left) and for ELP without RGD ligand (bottom). (c) Schematic demonstrating the high ligand density triggered by micelle formation when the temperature is increased above the CMT. (d) ELP signal (green) is observed intracellularly for Arg5 (ELP containing 5 arginines on the end of the polymer), micelle forming ELP above the CMT (iv and inset), but there is negligible signal for all samples below CMT (37°C, (i)–(iii) top), ELP without Arg5 ((ii) and (v) middle), and ELP that does not form micelles ((iii) and (vi) right). Scale bars are 25 μm. Adapted from References 45 and 27. Note: *T*-temperature; BC, block copolymer; Arg, arginine; Gly, glycine; Asp, aspartate.

to integrins, cell surface receptors that are important for cell adhesion. Integrins are commonly overexpressed on tumor cells and on the blood vessels of tumors and therefore have been the target of many drug delivery strategies to date.[47–49]

Despite the overexpression of integrins in tumors, a single linear RGD peptide does not interact strongly enough with an integrin to significantly enhance uptake of the peptide.[46] However, if the ligand is presented in high density as on the corona—exterior—of a micelle, the interaction is much stronger because of multivalency, a phenomenon in which multiple ligands simultaneously interact with many closely clustered receptors—integrins in this case—on the cell surface. These multiple interactions lead to a greater overall affinity than a single RGD-integrin interaction (the overall affinity derived from multivalent interaction is termed "avidity") and significantly greater cell uptake. This is illustrated in Figure 7b, where a micelle-forming ELP that presents a RGD peptide at its hydrophilic terminus—and a control ELP missing the RGD peptide—are tested for internalization at temperatures below and above their CMT. The RGD-containing ELP has slightly greater uptake compared to its RGD negative control. However, when the temperature is raised above the CMT, a drastic increase in cell uptake is achieved, presumably because of multivalent interactions between the RGD peptides presented by the micelle and integrins that are clustered on the cell membrane (Figure 7b, top right).

This system can also be extended to cell penetrating peptides (CPPs), a class of arginine-rich peptides that, rather than targeting a specific ligand, improve cell uptake by non-specifically interacting with the negatively charged phospholipids (lipids with negatively charged phosphate groups) and proteoglycan components (heavily glycosylated proteins) that are present on all cell membranes.[27] An advantage of this approach is that CPPs can theoretically target any tumor type since they do not rely on overexpression of a specific receptor. On the other hand, this lack of specificity could mean drastic off-target uptake by normal tissues.

To solve this problem, MacEwan and Chilkoti relied on the observation that the CPP activity of oligoarginine peptides is highly dependent on the number of arginine (Arg) residues—when the number of Arg residues is five or less, little cell uptake is seen, whereas six or more sequential Arg results in high cell uptake.[50] Building off this observation, MacEwan built a temperature-triggered cell penetrating nanoparticle that consists of a diblock ELP that presents an Arg5 peptide (five arginines) on the end of its hydrophilic block. The ELP was

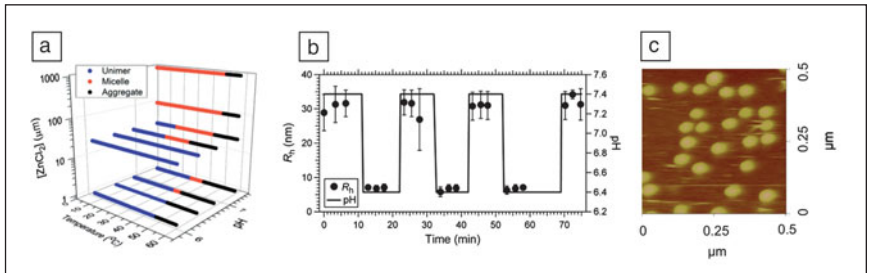


Figure 8. (a) Phase diagram of the triple-responsive (temperature, pH, and transition metal) micelles. Note that data in the absence of $ZnCl_2$ are plotted at 1 μM $ZnCl_2$ to enable presentation on a log scale. The different colored regions of the 3D plot represent the ranges of stimulus combinations (temperature, pH, and Zn^{2+} concentration) at which the histidine-rich diblock elastin-like polypeptide (ELP) exists as a unimer (blue), micelle (red), or aggregate (black). (b) pH triggered ELP self-assembly and disassembly. The left vertical axis shows the hydrodynamic radius (R_h), as measured by dynamic light scattering, while the right vertical axis shows the solution pH. The ELP repeatedly responds to cycles in pH by assembling into micelles (R_h of about 30 nm) at higher pH, and disassembling into unimers (R_h of 7–8 nm) at lower pH. (c) Triple responsive diblock ELPs self-assemble into spherical micelles as visualized by tapping mode atomic force microscopy in buffer.

https://doi.org/10.1557/mrs.2013.313 Published online by Cambridge University Press

designed through an iterative trial-and-error process to have a CMT of between 38–40°C. The hypothesis of this study was that at 37°C, micelle self-assembly cannot occur. The Arg5 presented by an ELP unimer would be insufficient to promote cell uptake, whereas at 42°C, a temperature above the CMT, the self-assembly of the ELP into spherical micelles would present a much higher local density of Arg residues that would confer CPP-like activity to the micelles, leading to significantly enhanced cell uptake (Figure 7c). Indeed, this hypothesis was proven to be correct, as shown in Figure 7d; raising the temperature from 37°C to 42°C drastically increased the cell uptake of the Arg5-ELP micelles (green, (i) and (iv)), but not for ELP micelles lacking the CPP segment ((ii) and (v)) or a single domain ELP that presents Arg5 but cannot undergo micellization because of its lack of amphiphilicity ((iii) and (vi)).

Triple responsive ELP micelles

The low tumor extracellular pH (6.2–6.9) is an interesting trigger that can be exploited to induce a material response solely in the tumor site for delivery of drugs and imaging agents.[51,52] Motivated by the prospect of ELP micelles that would respond to a pH trigger—the decrease in pH from the physiological pH of 7.4 to ~6.4—Callahan et al. synthesized an amphiphilic diblock ELP with histidine residues embedded in the hydrophobic ELP block.[53] They demonstrated that these ELPs are responsive to three stimuli: temperature, pH, and transition metals (**Figure 8**a). The histidine-rich hydrophobic segment results in the self-assembly of stable micelles at ~30°C at pH 7.4 that persist up to 40°C—beyond 40°C the micelles aggregate—such that they can be reversibly assembled by a thermal stimulus. They respond independently to pH, as lowering the pH from 7.4 to 6.4 ionizes the histidine residues, increasing the hydrophilicity of the core, abolishing the amphiphilicity of the polymer that drives the disassembly of the micelles into unimers (Figure 8b).[53] The transition metal coordination by histidine residues is the third trigger—coordination of Zn^{2+}, an ion that is present at micromolar concentrations in blood, stabilizes the micelles, as seen by the wider range of temperature over which the ELP remains assembled as micelles. This stabilization also decreases the concentration required to trigger micelle formation.

Next steps

The work reviewed herein shows the great potential of genetically engineered delivery systems. Using elastin-like polypeptides (ELPs) as an example, we show that such systems can meet the design criteria of scalability, biodegradability, monodispersity, targeting capability, and flexibility for a wide array of drugs. A great deal of functionality can be encoded into these systems at the genetic level such that complex and advanced capabilities are designed using simple and well-established DNA manipulation techniques.

While most functions—targeting, drug release, intracellular release, and trafficking—have genetically encodable parts available, the conjugation of drug to a genetically encodable peptide polymer carrier remains an exercise in organic and bioconjugate chemistry. This is because many cancer drugs are small and often hydrophobic small molecules, and our design strategy to create a nanoscale delivery system capitalizes on this feature to drive self-assembly of ELPs by conjugation of multiple copies of a hydrophobic drug site specifically to one end of the ELP (chimeric polypeptide-doxorubicin). The next crucial step is to eliminate this final drug conjugation step by exploiting the power of synthetic and chemical biology to encode the drug at the gene level. This development will allow us to create multifunctional nanoparticles by a "simplest to manufacture" purely genetically encoded design that is applicable to a range of small molecule drugs at a scale, cost, and reproducibility that will ease their translation to the clinic.

References

1. V. Wagner, A. Dullaart, A.-K. Bock, A. Zweck, *Nat. Biotechnol.* **24**, 1211 (2006).
2. M. Davis, Z. Chen, D. Shin, *Nat. Rev. Drug Discov.* **7**, 771 (2008).
3. T. Lammers, W. Hennink, G. Storm, *Br. J. Cancer* **99**, 392 (2008).
4. T. Allen, P. Cullis, *Science* **303**, 1818 (2004).
5. O. Koo, I. Rubinstein, H. Onyuksel, *Nanomed. Nanotechnol. Biol. Med.* **1**, 193 (2005).
6. G. Gregoriadis, *Ann. N.Y. Acad. Sci.* **308**, 343 (1978).
7. A. Rahman, A. Kessler, N. More, B. Sikic, G. Rowden, P. Woolley, P. Schein, *Cancer Res.* **40**, 1532 (1980).
8. A. Gabizon, D. Goren, Z. Fuks, A. Meshorer, Y. Barenholz, *Br. J. Cancer* **51**, 681 (1985).
9. M. Willis, E. Forssen, *Adv. Drug Deliv. Rev.* **29**, 249 (1998).
10. T. Lian, R. Ho, *J. Pharm. Sci.* **90**, 667 (2001).
11. D. Needham, G. Anyarambhatla, G. Kong, M. Dewhirst, *Cancer Res.* **60**, 1197 (2000).
12. A. Ponce, Z. Vujaskovic, F. Yuan, D. Needham, M. Dewhirst, *Int. J. Hyperthermia* **22**, 205 (2006).
13. H. Karanth, R. Murthy, *J. Pharm. Pharmacol.* **59**, 469 (2007).
14. A. Chilkoti, M. Dreher, D. Meyer, *Adv. Drug Deliv. Rev.* **54**, 1093 (2002).
15. T. Bin, X. Tao, T. Ren, Y. Weng, X. Lin, Y. Zhang, X. Tang, *J. Mater. Chem.* **22**, 17404 (2012).
16. D. Chow, M. Nunalee, D. Lim, A. Simnick, A. Chilkoti, *Mater. Sci. Eng., R* **62**, 125 (2008).
17. J. MacKay, M. Chen, J. McDaniel, W. Liu, A. Simnick, A. Chilkoti, *Nat. Mater.* **8**, 993 (2009).
18. B. Kim, A. Chilkoti, *J. Am. Chem. Soc.* **130**, 17867 (2008).
19. M. Dreher, W. Liu, C. Michelich, M. Dewhirst, A. Chilkoti, *Cancer Res.* **67**, 4418 (2007).
20. S. MacEwan, A. Chilkoti, *Biopolymers* **94**, 60 (2010).
21. D. Urry, C. Luan, T. Parker, D. Gowda, K. Prasad, M. Reid, A. Safavy, *J. Am. Chem. Soc.* **113**, 4346 (1991).
22. Y. Zhang, P. Cremer, *Curr. Opin. Chem. Biol.* **10**, 658 (2006).
23. J. McDaniel, D. Radford, A. Chilkoti, *Biomacromolecules* **14**, 2866 (2013).
24. W. Liu, M. Dreher, D. Furgeson, K. Peixoto, H. Yuan, M. Zalutsky, A. Chilkoti, *J. Control. Release* **116**, 170 (2006).
25. S. MacEwan, D. Callahan, A. Chilkoti, *Nanomedicine* **5**, 793 (2010).
26. M. Dreher, A.J. Simnick, K. Fischer, R.J. Smith, A. Patel, M. Schmidt, A. Chilkoti, *J. Am. Chem. Soc.* **130**, 687 (2008).
27. S. Macewan, A. Chilkoti, *Nano Lett.* **12**, 3322 (2012).
28. P. Wust, B. Hildebrandt, G. Sreenivasa, B. Rau, J. Gellermann, H. Riess, R. Felix, P.M. Schlag, *Lancet Oncol.* **8**, 487 (2002).
29. D. Peer, J.M. Karp, S. Hong, O.C. Farokhzad, R. Margalit, R. Langer, *Nat. Nanotechnol.* **2**, 751 (2007).
30. R. Duncan, *Nat. Rev. Drug Discov.* **2**, 347 (2003).
31. R. Sallach, V. Conticello, E. Chaikof, *Biotechnol. Progr.* **25**, 1810 (2009).
32. D. Meyer, A. Chilkoti, *Nat. Biotechnol.* **17**, 1112 (1999).
33. R. Webster, E. Didier, P. Harris, N. Siegel, J. Stadler, L. Tilbury, D. Smith, *Drug Metab. Dispos.* **35**, 9 (2007).
34. L. Seymour, Y. Miyamoto, H. Maeda, M. Brereton, J. Strohalm, K. Ulbrich, R. Duncan, *Eur. J. Cancer* **31**, 766 (1995).
35. L. Seymour, R. Duncan, J. Strohalm, J. Kopecek, *J. Biomed. Mater. Res.* **21**, 1341 (1987).
36. H. Choi, W. Liu, P. Misra, E. Tanaka, J. Zimmer, B. Itty Ipe, M. Bawendi, J. Frangioni, *Nat. Biotechnol.* **25**, 1165 (2007).

https://doi.org/10.1557/mrs.2013.313 Published online by Cambridge University Press

37. F. Yuan, M. Dellian, D. Fukumura, M. Leunig, D.A. Berk, V.P. Torchilin, R.K. Jain, *Cancer Res.* **55**, 3752 (1995).
38. J. McDaniel, J. Bhattacharyya, K. Vargo, W. Hassouneh, D. Hammer, A. Chilkoti, *Angew. Chem. Int. Ed.* **52**, 1683 (2013).
39. L. Bao, A. Haque, K. Jackson, S. Hazari, K. Moroz, R. Jetly, S. Dash, *Am. J. Pathol.* **178**, 838 (2011).
40. W. Straube, E. Klein, E. Moros, D. Low, R. Myerson, *Int. J. Hyperthermia* **17**, 48 (2001).
41. J. McDaniel, S. Macewan, M. Dewhirst, A. Chilkoti, *J. Control. Release* **159**, 362 (2012).
42. A. Simnick, M. Amiram, W. Liu, G. Hanna, M. Dewhirst, C. Kontos, A. Chilkoti, *J. Control. Release* **155**, 144 (2011).
43. S. Bhagwat, J. Lahdenranta, R. Giordano, W. Arap, R. Pasqualini, L. Shapiro, *Blood* **97**, 652 (2001).
44. R. Pasqualini, E. Koivunen, R. Kain, J. Lahdenranta, M. Sakamoto, A. Stryhn, R. Ashmun, L. Shapiro, W. Arap, E. Ruoslahti, *Cancer Res.* **60**, 722 (2000).
45. A. Simnick, C. Valencia, R. Liu, A. Chilkoti, *ACS Nano* **4**, 2217 (2010).
46. M. Mammen, S.-K. Choi, G. Whitesides, *Angew. Chem. Int. Ed.* **37**, 2755 (1998).
47. G. Mizejewski, *Proc. Soc. Exp. Biol. Med.* **222**, 124 (1999).
48. X. Chen, C. Plasencia, Y. Hou, N. Neamati, *J. Med. Chem.* **48**, 1098 (2005).
49. W. Arap, R. Pasqualini, E. Ruoslahti, *Science* **279**, 377 (1998).
50. P. Wender, D. Mitchell, K. Pattabiraman, E. Pelkey, L. Steinman, J. Rothbard, *Proc. Natl. Acad. Sci. U.S.A.* **97**, 13003 (2000).
51. K. Na, Y. Bae, *Pharm. Res.* **19**, 681 (2002).
52. E. Lee, K. Na, Y. Bae, *J. Control. Release* **91**, 103 (2003).
53. D. Callahan, W. Liu, X. Li, M. Dreher, W. Hassouneh, M. Kim, P. Marszalek, A. Chilkoti, *Nano Lett.* **12**, 2165 (2012). □

EMC
56th Electronic Materials Conference
June 25-27, 2014
University of California, Santa Barbara
Santa Barbara, CA

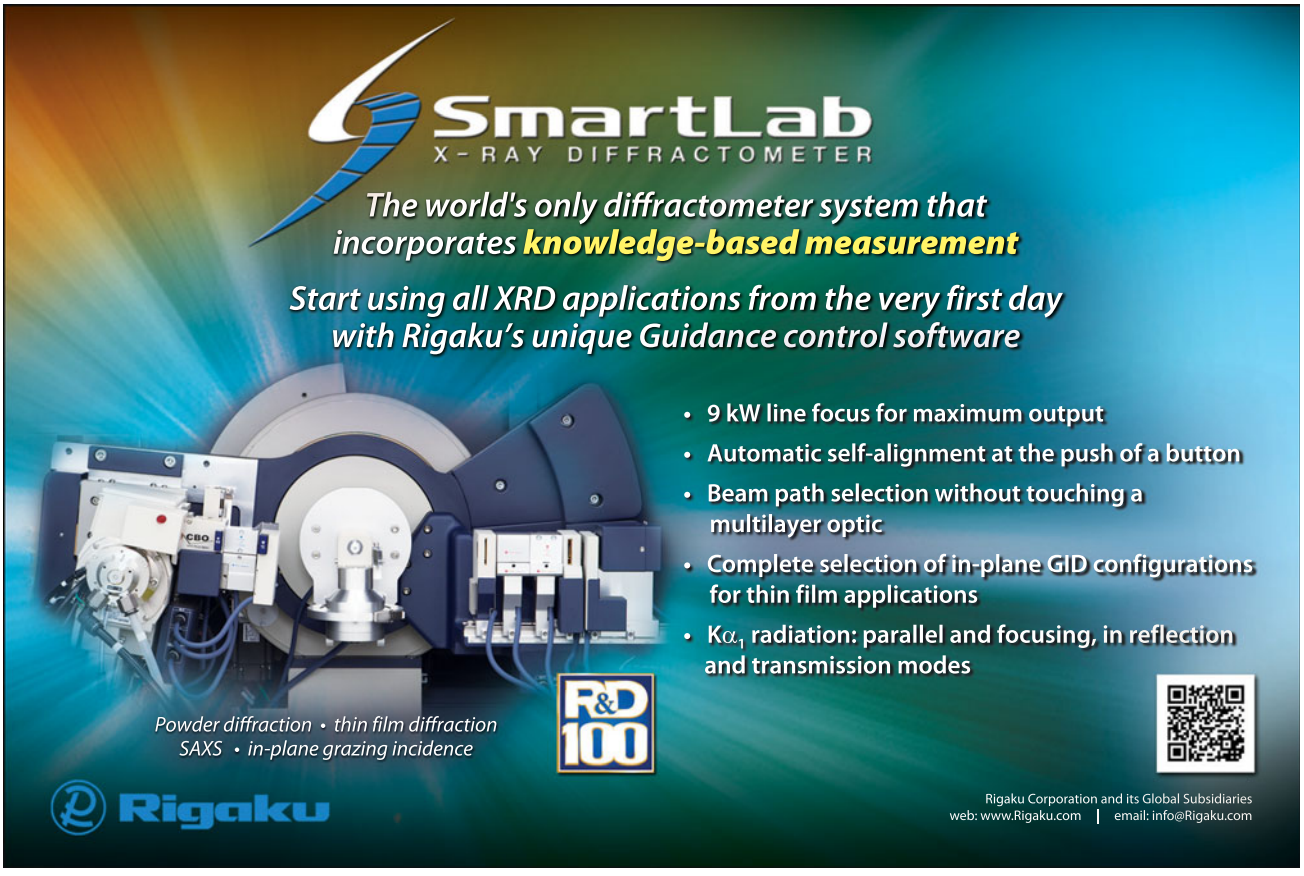
CALL FOR PAPERS

SCIENTIFIC PROGRAM
The three-day Conference will feature oral and poster presentations covering 32 topics in these 5 categories:
- ENABLING TECHNOLOGIES
- ENERGY CONVERSION AND STORAGE MATERIALS
- NANOSCALE SCIENCE AND TECHNOLOGY IN MATERIALS
- ORGANIC MATERIALS AND THIN FILM TECHNOLOGY
- WIDE BANDGAP MATERIALS

IMPORTANT DATES
Abstract Submission Ends
January 31, 2014
Preregistration Opens
Late February 2014
Preregistration Ends
Early June 2014

www.mrs.org/56th-emc

TMS FOUNDATION
Student participation in this Conference is partially supported by a grant from the TMS Foundation.



https://doi.org/10.1557/mrs.2013.313 Published online by Cambridge University Press